

Controllable Synthesis of Polyaniline Multidimensional Architectures: From Plate-like Structures to Flower-like Superstructures

Chuanqiang Zhou, Jie Han, and Rong Guo*

School of Chemistry and Chemical Engineering, Yangzhou University, Yangzhou, 225002 Jiangsu, P. R. China

Received January 8, 2008; Revised Manuscript Received June 1, 2008

ABSTRACT: Polyaniline multidimensional architectures from plate-like structures to flower-like superstructures have been successfully tailored by the oxidation polymerization in dilute aniline solution at room temperature, when the molar ratio of oxidant to monomer was altered in the range of 0.1:1–0.8:1. It was found that at low molar ratio (0.1:1–0.3:1) plate-like structures could be synthesized, while the as-synthesized product at the higher molar ratio (0.4:1–0.8:1) was flower-like superstructures; and the effect of monomer concentration on the shape of plate-like or flower-like architectures was also investigated. More importantly, their growth processes have been followed by measuring the morphological evolutions and chemical structures of products with the different reaction times, and then a plausible interpretation to their formation was brought forward through discussing the polymerization courses at two molar ratios (0.2:1 and 0.6:1). Besides, the molecular weight and conductivity of products obtained were also measured in this report.

Introduction

As one of the most widely investigated conducting polymers, polyaniline (PANI) has attracted considerable attention owing to its ease of synthesis, stability in ambient conditions, and relatively high levels of electrical conductivity.¹ And many studies have lately focused on PANI nanostructures because the high surface area of the material was of interest for the development of improved sensors and catalytic materials.² A variety of chemical methods have been employed to synthesize one-dimensional (1D) nanostructures of PANI such as tubes, belts, and fibers. Examples include template directed synthesis,³ the introduction of surfactants⁴ or seeds,⁵ interfacial polymerization,⁶ and rapidly mixed polymerization.⁷ In comparison with 1D nanostructures, the multidimensional (MD) architectures of conducting polymer possibly provided a great deal of opportunity to explore their novel properties due to their complex architectures. In fact, MD architectures such as nanoplates or flower-like architectures were believed to have a marvelous ability to control physical and chemical properties.⁸ Therefore, finding a mild and operated synthetic approach to PANI MD architectures⁹ represents a significant challenge in the field of controllable assembly of conducting polymers nanostructures so far.

In the chemical synthesis various oxidants, such as ammonium peroxydisulfate (APS),^{4–7,9,10} chloraurate acid,¹¹ ferric chloride,¹² horseradish peroxidase,¹³ and vanadic acid,¹⁴ have been employed to adjust the molecular structures and physical properties of PANI nanostructures. Of these oxidants, APS as a familiar reagent was used to initiate the oxidation polymerization of aniline for synthesizing PANI. Recently, Stejskal and co-workers have investigated the effect of APS amount on the yield and conductivity of resulting PANI.¹⁵ However, the reports on the fabrication of PANI nanostructures at varying APS/aniline ratio and mild ambient conditions (such as room temperature), to the best of our knowledge, were very sparse yet. In this report, we systematically investigate the morphological dependence of product on the molar ratio of APS to aniline between 0.1:1 and 0.8:1 at room temperature. Especially, the plate-like structures and flower-like superstructures can be harvested under the [APS]/[aniline] ratios of 0.2:1 and 0.6:1, respectively, and their

growth processes are also observed using an electron microscope and FTIR technologies. The concentration of aniline used in our experiments is low, e.g., ~32 mM, compared with that used in the conventional synthesis, e.g., ~200 mM of aniline,¹⁶ which is also discovered to be crucial to successfully tailor the MD architectures of PANI.

Experimental Section

Materials. Aniline monomer (Shanghai Chemical Co.) was distilled under reduced pressure. APS ((NH₄)₂S₂O₈, Shanghai Chemical Co.) and other reagents were used as received.

Synthesis of PANI. In a typical synthesis, 0.060 g of aniline was dispersed in 20 mL of deionized water with magnetic stirring at room temperature for 5 min to obtain a uniform solution. The aqueous solution of ammonium persulfate (APS) was added to the above mixture, and the resulting solution was stirred for another 0.5 min to ensure complete mixing. And then the reaction was allowed to proceed without agitation for 24 h at 25 °C. Finally, the products were washed with deionized water until the filtrate became colorless and dried in a vacuum at 60 °C for 24 h.

Characterization. The morphologies of products were examined by a field-emission scanning electron microscope (FESEM, S-4800, Hitachi Co., Japan) and a transmission electron microscope (TEM, Tecnai-12 Philip Apparatus Co.). The FTIR spectra (Nicolet-740) were recorded in the range of 400–4000 cm⁻¹. The UV–vis spectrum (UV-250, Shimadzu Corp., Japan) of sample dissolved in water was measured in the range between 320 and 900 nm. The molecular weights of as-synthesized products dissolved in *N,N'*-dimethylformamide (DMF) were measured with gel permeation chromatography (GPC, Agilent 1100, Agilent Co.). Before analysis, the sample was filtered through a 0.45 μm syringe filter, and DMF was used as the eluent with the flow rate of 1 mL min⁻¹ at 25 °C. Calibration was accomplished with monodisperse polystyrene standards. The conductivity of product was measured by a tow-point technique on pellets from polymer powders at room temperature.

Results and Discussion

Morphology. Figure 1 exhibits the FESEM images of plate-like structures synthesized with the [APS]/[aniline] ratio varying in the range of 0.1:1–0.3:1. It is clearly observed from Figure 1A,B that the product is composed of a large amount of 2D plate-like structures close to disks (about 100 nm in thickness

* Corresponding author. E-mail: guorong@yzu.edu.cn.

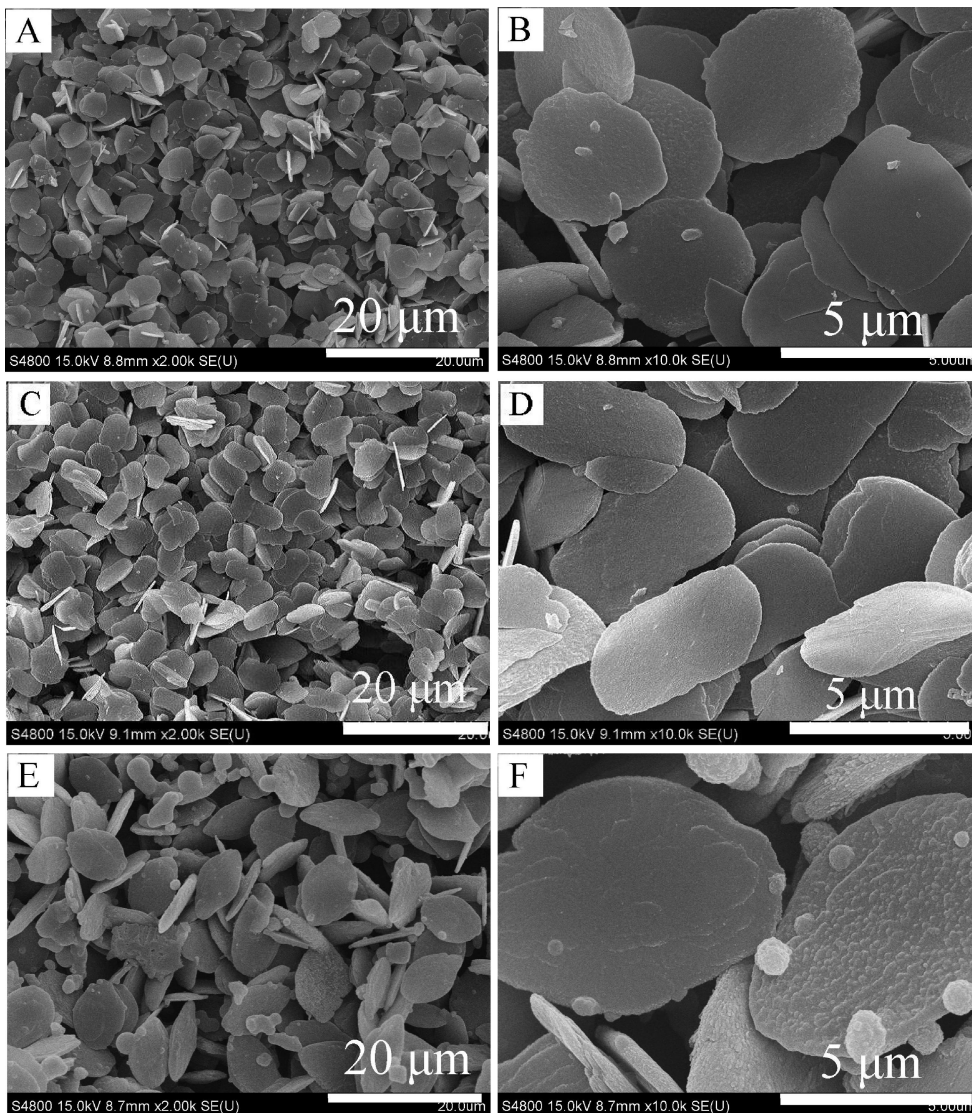


Figure 1. FESEM images of plate-like structures with the various [APS]/[aniline] ratios: (A, B) 0.1:1; (C, D) 0.2:1; (E, F) 0.3:1. Other synthetic conditions: [aniline] = 32 mM, 25 °C, 24 h.

and 3.5–4.5 μm in lateral diameter) at the ratio of 0.1:1, while the morphology of product obtained with 0.2:1 [APS]/[aniline] ratio is well-defined semirectangular plates with sleek forelands and smooth surfaces, which are 200 nm in thickness and 3.5–5.5 μm in lateral dimension (Figure 1C). From Figure 1D, one can find that these plate-like structures are fragile, and some broken plates appear in sample. At the molar ratio of 0.3:1, large rhombus plates (around 7 μm in short axis and 10 μm in long axis) decorated by some particulates are formed (Figure 1E,F). For these observations, it can be concluded that plate-like structures as a dominating morphology are obtained with the [APS]/[aniline] ratio varying between 0.1:1 and 0.3:1 and the aniline concentration of 32 mM.

However, when the polymerization reaction is performed with the higher molar ratio of oxidant to monomer (≥ 0.4), the morphology of product changes to 3D hierarchical architecture (flower-like superstructures), as shown in Figure 2. From Figure 2A,B, it is evidently seen that the flower-like architectures of PANI are harvested at 0.4:1 molar ratio, and they are made up of several wide petals covered by arranged particulates as illustrated in the inset of Figure 2B. As the [APS]/[aniline] ratio increasing to 0.6:1 (Figure 2C), the as-resultant product consists of uniform ca. 4.5 μm flower-like superstructures with high hierarchy assembled by several tens of petals (1.5 μm in length

and 1 μm in wide). Careful observation to Figure 2D discerns that these petals are arranged by quasi-parallel 1D nanostructure (such as nanofibers with 50 nm in diameter) which seem to fuse together or cross-link into mat-like structure as shown in the inset. With the higher molar ratio of 0.8:1 (Figure 2E,F), the petals of superstructures are seen to consist visibly of nanosheets with 70 nm in average thickness or are knitted by nanofibers with 50 nm in diameter, accompanied by the appearance of particles. If the molar ratio is altered to 1.0:1, the oxidation polymerization of aniline in such system produces nanotubes of PANI, which is identical to the result reported by Stejskal.^{10a,16}

Notably, our preliminary experiments indicate that the morphology and size of plate-like structures are dependent on the concentration of aniline keeping the [APS]/[aniline] ratio (0.2:1) unchanged, as shown in Figure 3. When the concentration of aniline is relatively low (such as 20 mM), there are a lot of small-sized disk-shape plates of PANI with 3.2 μm in mean diameter seen in sample, accompanied by few large-sized irregular plates (Figure 3A). However, as the concentration of aniline increases to 28 mM (Figure 3B), the shape of plate changes to semirectangular aspect, whose shorter and longer edges are 3.5 and 5.5 μm , respectively, while they are apart 4 and 6 μm at the aniline concentration of 44 mM (Figure 3C).

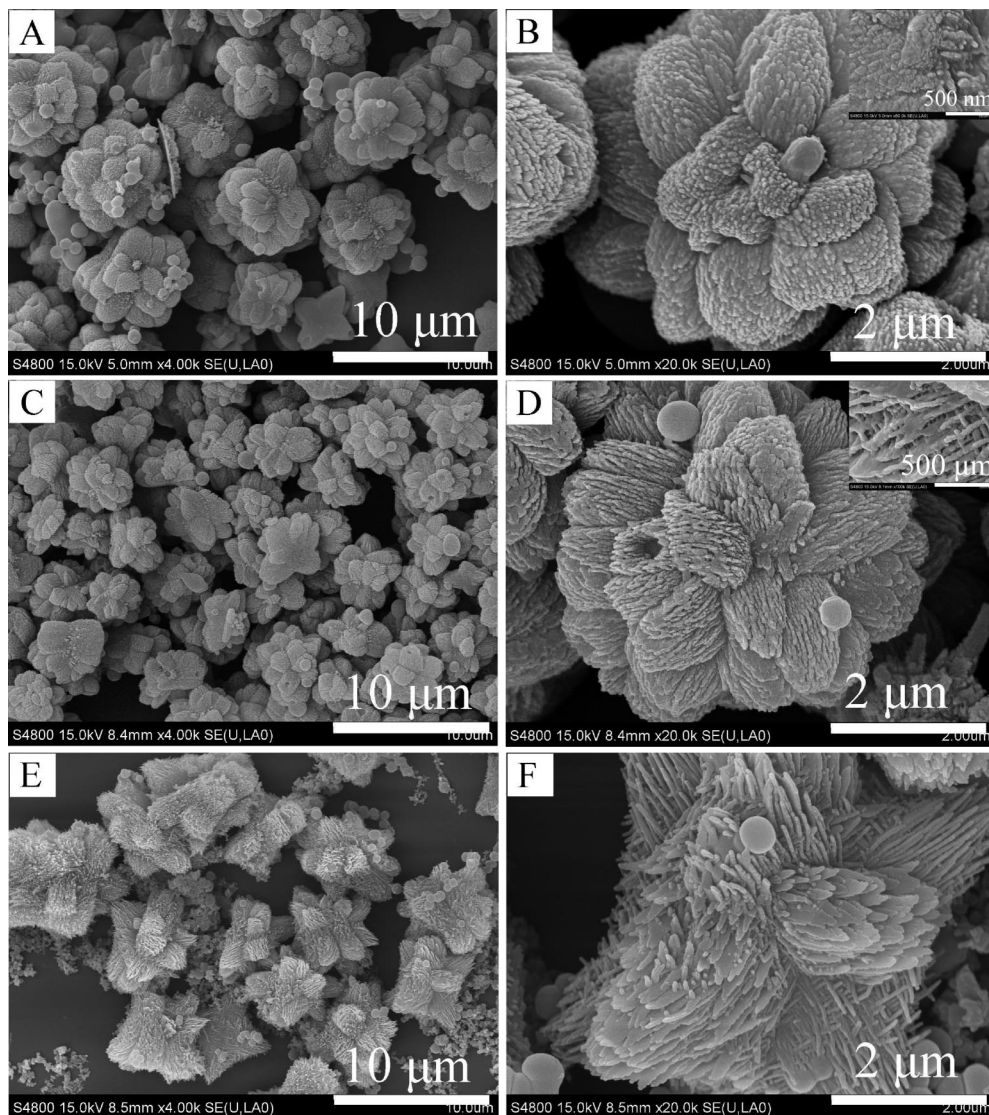


Figure 2. FESEM images of PANI flower-like superstructures with the different [APS]/[aniline] ratios: (A, B) 0.4:1; (C, D) 0.6:1; (E, F) 0.8:1. Other synthetic conditions: [aniline] = 32 mM, 25 °C, 24 h.

Figure 3D displays that these resultant plates of PANI become larger in dimensions (about $4.5\ \mu\text{m}$ in shorter edges and $7\ \mu\text{m}$ in longer edges), and their forelands seem to be broken with the higher concentration of 50 mM. For each sample, the standard deviation of lateral size is typically within 10% when measured from more than 100 plates by FESEM imaging. In fact, at the [APS]/[aniline] ratio of 0.6:1, the morphology of as-obtained flower-like superstructures is also influenced by the concentration of aniline. We find that the morphology of product synthesized at the aniline concentration of 24 mM (Figure 4A) is basically similar to that in Figure 2D; however, as the concentration of aniline increases to 40 mM (Figure 4B), the petals of flower-like structures change to mat-like structures knitted by crossed nanofibers, and their number for assembling into flower-like architectures reduces to 3–5.

Growth Processes. To quench the polymerization as soon as possible, a small amount of reaction extract is quickly diluted to the optimal concentration for TEM experiments and deposited immediately onto sample grids placed on a piece of filter paper.¹⁷ In this way, the products with different reaction stages are obtained for examining the morphological evolution and chemical structures of products to reveal their growth processes. Figure 5 gives TEM and FESEM (insets) images of products prepared at the [APS]/[aniline] ratio of 0.2:1 after the reaction

of 10, 20, 30, and 50 min. As short as 10 min (Figure 5A), product with a rhombus morphology forms in solution, while the truncated rhombus plates appear in product after another 10 min (Figure 5B). With the reaction continuing to 30 min, those truncated rhombus plates evolve into approximate hexagonal plates (Figure 5C). As they further grow, the hexagonal plates gradually develop to elliptic plates with four sleek forelands when the reaction time is prolonged to 50 min (Figure 5D). From these observed results, it is clear that the rhombus plates as primordial morphology form at first, then evolving gradually into truncated rhombus plates and hexagonal plates, and finally semirectangular plates.

Besides, Figure 6A gives the FTIR spectra of products with the reaction times of 10, 30, and 50 min, which is expected to provide information on the chemical structures of these products. At first, the curve “10 min” shows the unfamiliar peaks marked in Figure 6A, which should be assigned to phenazine segment in product. For example, the band at $1625\ \text{cm}^{-1}$ corresponds to the absorption of the C=C ring stretching vibration in substituted phenazine-like segments,¹⁶ and the band observed at $1404\ \text{cm}^{-1}$ is attributable to a totally symmetric stretching of the phenazine heterocyclic ring.¹⁸ According to ref 16, phenazines can also be recognized through the bands at $1208\ \text{cm}^{-1}$ ($1192\ \text{cm}^{-1}$ in spectrum) and by their contribution to the bands at $1108\ \text{cm}^{-1}$

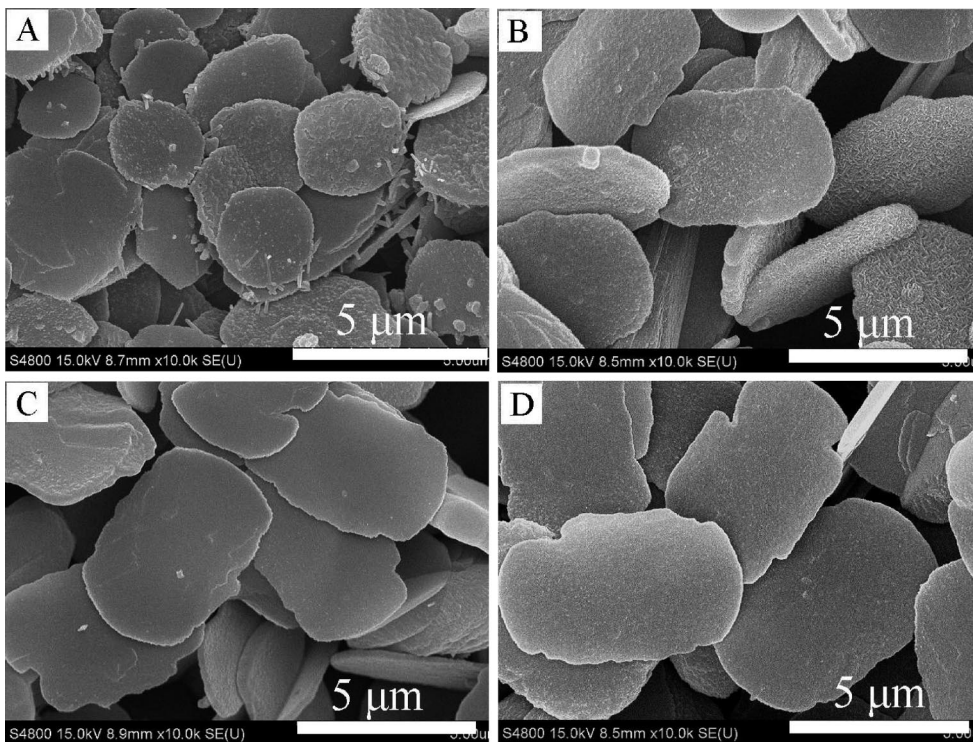


Figure 3. FESEM images of PANI plate-like structures synthesized with different concentrations of aniline (mM): (A) 20, (B) 28, (C) 44, and (D) 50. Other synthetic conditions: [APS]/[aniline] = 0.2:1, 25 °C, 24 h.

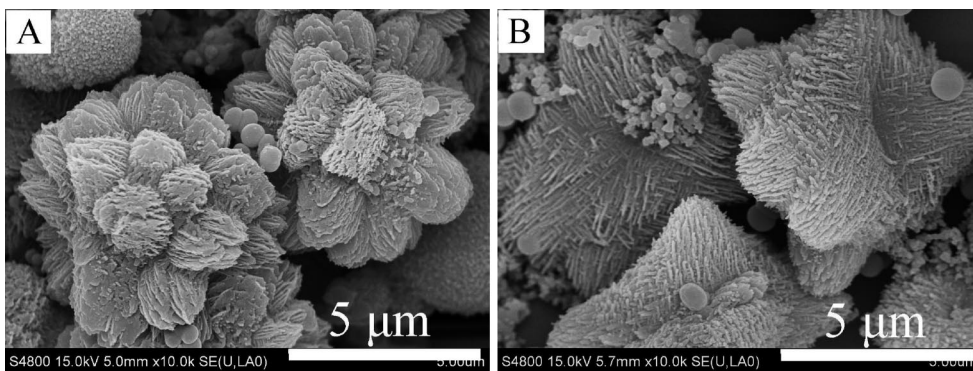


Figure 4. FESEM images of PANI flower-like superstructures synthesized with different concentrations of aniline (mM): (A) 24; (B) 40. Other synthetic conditions: [APS]/[aniline] = 0.6:1, 25 °C, 24 h.

(1112 cm^{-1} in spectrum) and 1144 cm^{-1} ; however, the band at 1144 cm^{-1} on the curve “10 min” in Figure 6A is overlapped by neighboring adsorption. In addition, the UV-vis spectrum in Figure 6B shows a strong absorption at 420 nm, which should be assigned to the $\pi-\pi^*$ transition associated with phenazine units conjugated to lone pairs of bridging nitrogen,¹⁹ further attesting to the appearance of the phenazine segment in offspring at the reaction time of 10 min. These observations could indicate that the oligomers produced at the beginning of polymerization ought to contain phenazine segment, which are generally derived from the ortho coupling of aniline constitutional units as a importance linkage in the induction period of reaction.²⁰ Also, one can also find that these peaks attributable to phenazines weaken in intensity with the reaction time prolonging from 10 to 50 min, indicative of their decreasing proportion in product. Simultaneously, as the reaction proceeds, these characteristic bands due to a conventional PANI chains, such as 1583, 1507, 1444, and 1300 cm^{-1} marked in the curve “50 min”, become stronger, as compared to these three spectra. This suggests that after the induction period, as expected, aniline molecules are

still chained in the para position of oligomers as a main coupling mode in conventional chains.

Again, the corresponding time-dependent evolution of flower-like superstructures is also recorded by FESEM at the [APS]/[aniline] ratio of 0.6:1 in the same manner, as the result displayed in Figure 7. At the early stages of 25 min, the as-synthesized product is composed of ca. 2.5 μm flower-like architectures assembled from radially rhombus leaves (Figure 7A), which are discovered to have cortex-like surface seen from the inset. As the reaction time increases to 45 min (Figure 7B), the honeycomb-like superstructures covered by squama-like nanostructures are seen in product. However, petals of flower-like architectures are arranged by these ordered quasi-parallel nanofibers when it is 1 h (Figure 7C). After another 3 h, these petals become longer (ca. 2 μm in length), and their building blocks evolve into approximate nanosheets (Figure 7D). At the initial stage of reaction before 25 min, the newly produced precipitate is too little to gather for the FESEM observation, whereas TEM is employed to examine product produced at 15

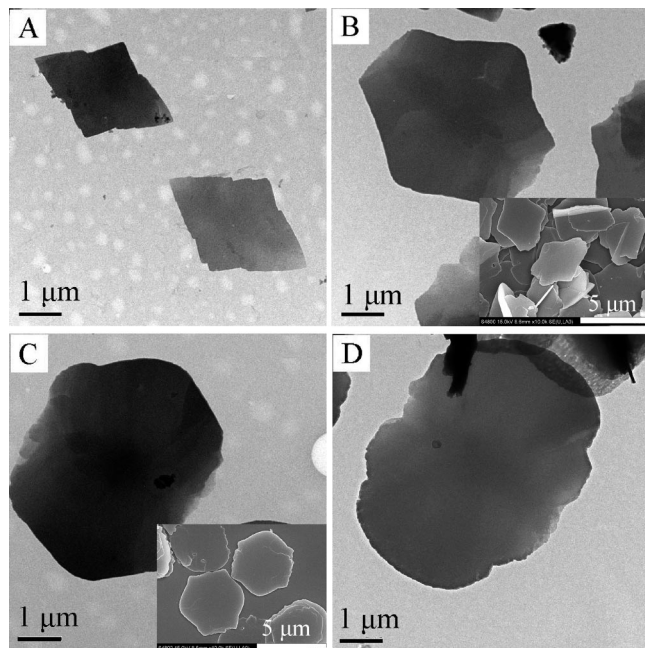


Figure 5. TEM and FESEM (insets) images of plates synthesized with different reaction times (min): (A) 10, (B) 20, (C) 30, and (D) 50. Synthetic conditions: [aniline] = 32 mM, [APS]/[aniline] = 0.2:1, 25 °C.

min and gives the morphology of rhombus plates similar to that shown in Figure 5A.

Moreover, from the FTIR spectra exhibited in Figure 8, it can be seen that the intensity of the band at 858 cm^{-1} corresponding to 1,4-substitution of aromatic rings depresses as the [APS]/[aniline] ratio is more than 0.4:1, meaning the decreasing proportion of such structure in polymer chains. In contrary, 1,2,4-substitution of the aromatic ring which is commonly generated by the cross-linking reaction among polymer chains shows an increasing trend in polymer chains with the ratio more than 0.4:1, which can be validated by the appearance and strengthening of the band at 1041 cm^{-1} .²¹ In other words, the cross-linking reaction among chains occurs when the [APS]/[aniline] ratio is more than 0.4:1, accompanied by the formation of flower-like superstructures (Figure 2). Therefore, it is reasonable to believe it is the cross-linking reaction that guides the growth of polymer chains, inducing the assembly of flower-like architectures.

Formation Mechanism. The pH values of reaction systems with two different [APS]/[aniline] ratios (0.2:1 and 0.6:1) are monitored apart to discuss the polymerization processes of aniline, and the results are shown in Figure 9. It is found that after the addition of oxidant APS the pH values of both solutions decrease with the polymerization reaction proceeding, which is due to that hydrogen atoms abstracted from amino groups and benzene rings during the oxidation, are released as protons.²² Obviously, the decreasing tendency at the [APS]/[aniline] ratio of 0.6:1 is more apparent than that at the 0.2:1 ratio because of the more oxidant used. Since the pK_a of aniline is reported to be 4.9,²⁰ the polymerization at 0.2:1 ratio of [APS]/[aniline] takes place in weak acidic condition ($\text{pH} > 5.0$) during the reaction course; thus, aniline exists as a lot of neutral molecules which are easily oxidized and less anilinium cations which are oxidized much more slowly.¹⁶ Quantum chemical calculations suggest that besides the prevalent para-coupling of aniline molecules, the oxidation reaction started in weak acid medium also produces 2-aminodiphenylamines by coupling in the ortho-position; after the trimerization process, the ortho-coupling structures of oligomer chains could be further oxidized to

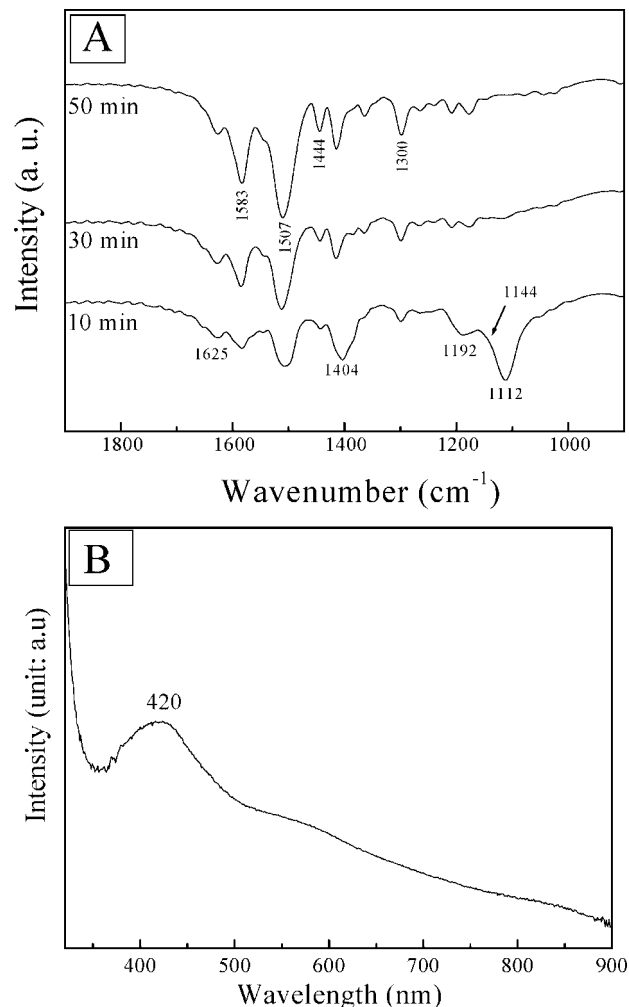


Figure 6. (A) FTIR spectra of products synthesized with different reaction times (min): 10; 30; 50. (B) UV-vis spectrum of offspring synthesized with the reaction time of 10 min. Synthetic conditions: [aniline] = 32 mM, [APS]/[aniline] = 0.2:1, 25 °C.

substituted phenazines through an intramolecular cyclization reaction.^{20,23} Such phenazine segments in oligomer chains of product is revealed as mentioned above (Figure 6A), and their low solubility in water and flat geometrical structures may result in their precipitation in two dimensionality,^{9b} such as rhombus plates (Figure 5A). After that, these insoluble oligomer intermediates (plates) generated during the early stages of polymerization would play a template to guide the growth of supramolecular structures²³ and evolve into elliptic plates as a final morphology (Figure 5B–D). The exact reason on the formation of rhombus plates originally yielded is still unclear; however, the morphological evolvement from rhombus to elliptic plates might be deemed as a thermodynamically favorable process.²⁴

As for the [APS]/[aniline] molar ratio of 0.6:1, the time dependence experiment of morphological evolution discussed above illustrates that the flower-like architectures originate from the self-assembly of rhombus plates through the cross-linking reaction (Figure 8). From the Figure 9, it is also seen that the pH value of reaction system at the 0.6:1 ratio decreases as aniline polymerizes and is lower than 4.9 (the pK_a of aniline) after the polymerization time of 56 min when the anilinium cation becomes the prominent monomer form. With the polymerization of anilinium cations, the nanofibers seem to be a basic morphological units of product^{6,7} and Figure 7C with the reaction time of 60 min (1 h) exhibits the presence of nanofibers

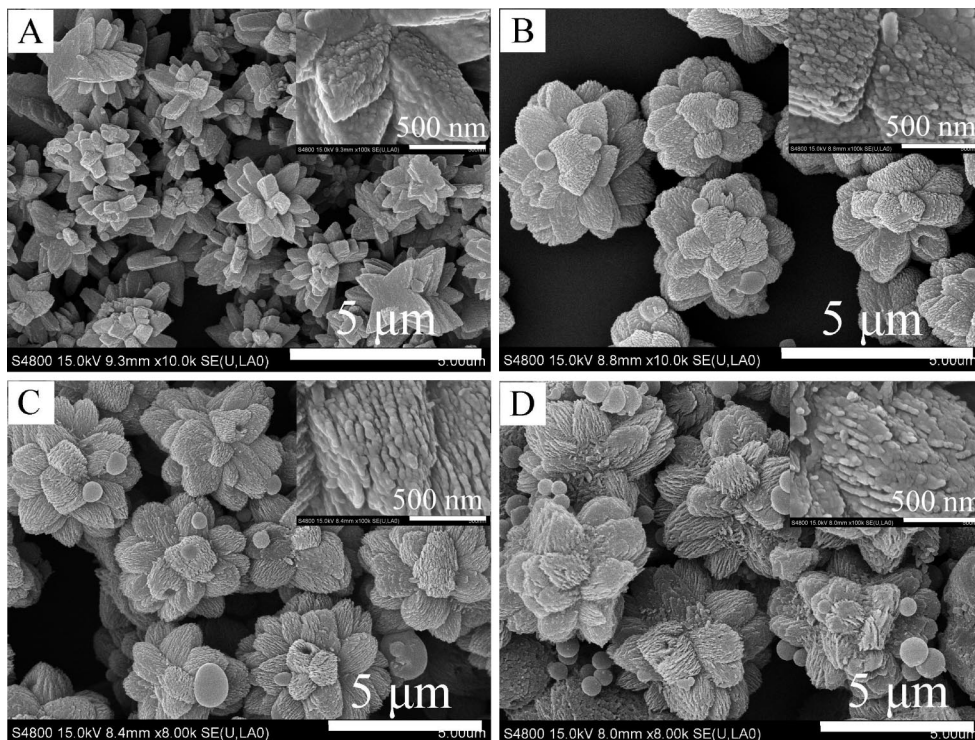


Figure 7. FESEM images of offspring synthesized with different reaction times: (A) 25 min; (B) 45 min; (C) 1 h; (D) 4 h. Synthetic conditions: [aniline] = 32 mM, [APS]/[aniline] = 0.6:1, 25 °C.

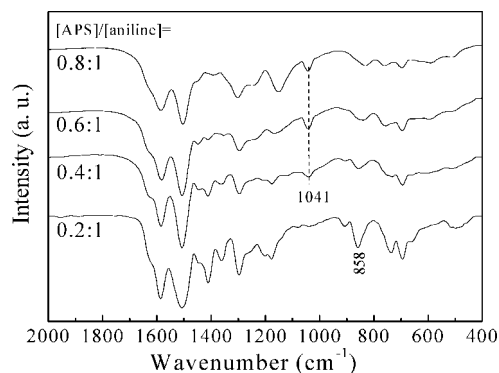


Figure 8. FTIR spectra of PANIs synthesized at different molar ratios of APS to aniline (marked in this figure), other synthetic conditions: [aniline] = 32 mM, 25 °C, 24 h.

on the flower-like superstructures, further accounting for this fact.

GPC Analysis and Conductivity. The GPC experiment was performed to determine the molecular weight of offspring. It is found that the number-average molecular weights of products synthesized with the low ratio of APS to aniline (0.1:1 and 0.8:1) are 1091 and 6844 with the polydispersity 1.21 and 1.03, respectively. One can see from these results that the molecular weights of products are relative low in comparison with the conventional PANI prepared at 1.25:1 of [APS]/[aniline] ratio (tens of thousands).²⁵ Similarly, because of the limited oxidant amount, the room conductivity of products also is quite low ($<10^{-10}$ S cm^{-1}) with the [APS]/[aniline] ratio varying from 0.1:1 to 0.8:1 even if after doping with 1.0 M HCl aqueous solution. The reduced conductivity results from this fact: The less oxidant is depleted in the early stages of oxidation, which usually yields oligoaniline containing ortho-coupling of aniline units besides para-linkage; as a consequence, the as-synthesized product is nonconductivity and cannot be protonated by protonic acid because of the nonconjugated system.¹⁶ In the past years,

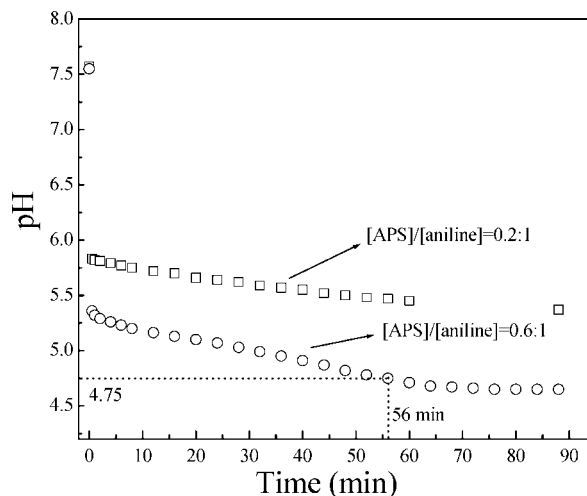


Figure 9. pH value of solution decreasing as aniline polymerizes due to released protons. Other conditions: [aniline] = 32 mM, 25 °C, 24 h.

the conductivity was the main goal of researches in the field of aniline polymerization. However, very recently, the nanoscale morphology of the products was becoming an important and interesting object in this field due to the potential future technology in micro/nanoscience.²⁵

Conclusion

The fabrication of polyaniline plate-like structures and flower-like hierarchical superstructures has been successfully realized when the oxidation polymerization of aniline were carried out in dilute solution with the oxidant/monomer molar ratio varying between 0.1:1 and 0.8:1. The low molar ratio (0.1:1–0.3:1) results in the plate-like structures of polyaniline, while the higher molar ratio (0.4:1–0.8:1) can yield flower-like architectures. The 0.2:1 and 0.6:1 of oxidant/monomer molar ratio are chosen

to investigate the growth processes of plate-like and flower-like architectures, respectively. By performing the time-dependent experiments and monitoring the pH value changes of two reaction systems, we deduce the polymerization processes and propose a plausible interpretation to the formation of plate-like and flower-like architectures. And the molecular weight and conductivity of offspring are also measured in order to better understand the products. This room-temperature and lowering-oxidant strategy is very simple, mild and controllable, which presents a new approach for the fabrication of conducting polymer multidimensional or hierarchical nanostructures.

Acknowledgment. This work was supported by the National Natural Scientific Foundation of China (No. 20633010 and 20773106).

References and Notes

- (1) Cao, Y.; Smith, P.; Heeger, A. J. *Synth. Met.* **1992**, *48*, 91–97.
- (2) Berdichevsky, Y.; Lo, Y. H. *Adv. Mater.* **2006**, *18*, 122–125.
- (3) Wu, C. G.; Bein, T. *Science* **1994**, *264*, 1757–1759.
- (4) Zhang, Z.; Wei, Z.; Wan, M. *Macromolecules* **2002**, *35*, 5937–5942.
- (5) Zhang, X.; Goux, W. J.; Manohar, S. K. *J. Am. Chem. Soc.* **2004**, *126*, 4502–4503.
- (6) Huang, J.; Virji, S.; Weiller, B. H.; Kaner, R. B. *J. Am. Chem. Soc.* **2003**, *125*, 314–315.
- (7) Huang, J.; Kaner, R. B. *Angew. Chem., Int. Ed.* **2004**, *43*, 5817–5821.
- (8) Jiang, L. P.; Xu, S.; Zhu, J. M.; Zhang, J. R.; Zhu, J. J.; Chen, H. Y. *Inorg. Chem.* **2004**, *43*, 5877–5883.
- (9) (a) Han, J.; Song, G.; Guo, R. *Adv. Mater.* **2007**, *19*, 2993–2999. (b) Zhou, C.; Han, J.; Song, G.; Guo, R. *Macromolecules* **2007**, *40*, 7075–7078.
- (10) (a) Trchová, M.; Šeděnková, I.; Konyushenko, E. N.; Stejskal, J.; Holler, P.; Čirić-Marjanović, G. *J. Phys. Chem. B* **2006**, *110*, 9461–9468. (b) Li, G.; Zhang, Z. *Macromolecules* **2004**, *37*, 2683–2685.
- (11) Wang, Y.; Liu, Z.; Han, B.; Sun, Z.; Huang, Y.; Yang, G. *Langmuir* **2005**, *21*, 833–836.
- (12) Zhang, L.; Wan, M.; Wei, Y. *Macromol. Rapid Commun.* **2006**, *27*, 366–371.
- (13) Ma, Y.; Zhang, J.; Zhang, G.; He, H. *J. Am. Chem. Soc.* **2004**, *126*, 7097–7101.
- (14) Li, G.; Jiang, L.; Peng, H. *Macromolecules* **2007**, *40*, 7890–7894.
- (15) Blinova, N. V.; Stejskal, J.; Trchová, M.; Prokeš, J.; Omastová, M. *Eur. Polym. J.* **2007**, *43*, 2331–2341.
- (16) Stejskal, J.; Sapurina, I.; Trchová, M.; Konyushenko, E. N.; Holler, P. *Polymer* **2006**, *47*, 8253–8262.
- (17) Huang, J.; Kaner, R. B. *Chem. Commun.* **2006**, 367–376.
- (18) (a) Viva, F. A.; Andrade, E. M.; Molina, F. V.; Florit, M. I. *J. Electroanal. Chem.* **1999**, *471*, 180–189. (b) Dines, T. J.; MacGregor, L. D.; Rochester, C. H. *Phys. Chem. Chem. Phys.* **2001**, *3*, 2676–2685.
- (19) (a) Premasiri, A. H.; Euler, W. B. *Macromol. Chem. Phys.* **1995**, *196*, 3655–3666. (b) Valle, M. A. del.; Díaz, F. R.; Bodini, M. E.; Alfonso, G.; Soto, G. M.; Borrego, E. D. *Poly. Int.* **2005**, *54*, 526–532. (c) Gautot, J. E.; Hodge, P. *Polymer* **2007**, *48*, 7065–7077.
- (20) Čirić-Marjanović, G.; Trchová, M.; Stejskal, J. *Collect. Czech. Chem. Commun.* **2006**, *71*, 1407–1426.
- (21) Tang, J. S.; Jing, X. B.; Wang, B. C.; Wang, F. S. *Synth. Met.* **1988**, *24*, 231–238.
- (22) (a) Fu, Y.; Elsenbaumer, R. L. *Chem. Mater.* **1994**, *6*, 671–677. (b) Neoh, K. G.; Kang, E. T.; Tan, K. L. *Polymer* **1993**, *34*, 3921–3928.
- (23) Čirić-Marjanović, G.; Trchová, M.; Stejskal, J. *Int. J. Quantum Chem.* **2008**, *108*, 318–333.
- (24) Xiong, Y.; Xia, Y. *Adv. Mater.* **2007**, *19*, 3385–3391.
- (25) Stejskal, J.; Sapurina, I.; Trchová, M.; Konyushenko, E. N. *Macromolecules* **2008**, *41*, 3530–3536.

MA800500U